The Journal of Experimental Biology **199**, 869–882 (1996)
Printed in Great Britain © The Company of Biologists Limited 1996
JEB0042

RETINAL DEVELOPMENT AND VISUAL SENSITIVITY OF YOUNG PACIFIC SOCKEYE SALMON (*ONCORHYNCHUS NERKA*)

IÑIGO NOVALES FLAMARIQUE AND CRAIG W. HAWRYSHYN
University of Victoria, Department of Biology, PO Box 1700, Victoria, British Columbia, Canada, V8W 2Y2

Accepted 19 December 1995

Summary

The development of photoreceptor cell types and the visual sensitivity of young sockeye salmon were examined. In contrast to previous findings from rainbow trout, rod outer segments were observed in the embryo 1.5 weeks before hatching. At this stage, a full square mosaic with accessory corner cones was visible in the central retina. Post-hatching retinal development is similar to that of other fish species. During the first 11 months of development, the fibrous and interplexiform layers, the outer nuclear layer, the visual cell layer and the retinal pigment epithelium thicken. The ganglion cell layer and the inner nuclear layer regress. In addition, the mean diameter of the cones increases, with that of double cones increasing faster than that of either of the single cone types. As is the case for other salmonids, the density of accessory corner cones diminishes after smoltification (a developmental stage in salmonids). The retina of smolts exhibits a full square mosaic pattern in some peripheral areas and near the central embryonic fissure. However, unlike findings from rainbow trout, compound action potential recordings from the optic nerve of smolt sockeye reveal the presence of four cone mechanisms with sensitivity maxima at 380 (ultraviolet), 425 (short), 520 (middle) and 635 nm (long wavelength). There is also a rod mechanism with maximum sensitivity around 530 nm. Smolts also exhibit polarization sensitivity to 380 nm light under a white crepuscular background.

Key words: sockeye salmon, *Oncorhynchus nerka*, retina, development, spectral and polarized light, sensitivities, ultraviolet cones.

Introduction

Retinal development in some fish species appears to differ from that of higher vertebrates in two major ways. These are (1) the delayed maturation of rods after hatching (Raymond, 1985; Hagedorn and Fernald, 1992), as opposed to their delayed appearance in higher vertebrates before birth (in general, cones appear before rods in both lower and higher vertebrates, but hatching may not be the equivalent to birth in terms of retinal development; Reh, 1991; Carter-Dawson and La Vail, 1979), and (2) the age-dependent density of accessory cones presumed to be sensitive to ultraviolet light (Bowmaker and Kunz, 1987; Hawryshyn *et al.* 1989; Loew and Wahl, 1991; Beaudet *et al.* 1993). One major group of fish possessing this second feature is the salmonids, family Salmonidae (Lyall, 1957; Kunz, 1987; Beaudet *et al.* 1993), which also possess cone combinations maximally sensitive to short- (blue), middle- (green) and long-wavelength (red) radiation (Bowmaker and Kunz, 1987; Kusmic *et al.* 1993; Hawryshyn and Hárosi, 1994).

The development of salmonid retinas was first studied using light microscopy (Lyall, 1957; Ali, 1959). These authors classified photoreceptor types and described trends in the growth of several retinal layers (Lyall, 1957; Ali, 1959). Although the reported growth trends were later supported by studies on other fish species (Blaxter, 1975; Ali and Wagner, 1980), additional photoreceptor types have since been found in early ontogeny of salmonids. For instance, reports describing the absence of rods at hatching among *Oncorhynchus* and *Salmo* species (Ali, 1959, 1963) differ from more recent findings using transmission electron microscopy (TEM) on rainbow trout (Schmitt and Kunz, 1989). In addition, previous light microscopy studies did not reveal any clear distinction between cone photoreceptor types at the embryonic and early post-hatching developmental stages (Lyall, 1957). Hence, the presence of accessory corner cones at these stages in salmonids has not been established [see radial sections in Schmitt and Kunz (1989) up to 3–4 weeks post-hatching, stages 1–3 in the eleutheroembryo (Balon, 1975)].

However, a number of recent findings have suggested that accessory corner cones may be important in the life of planktivorous fish and they are therefore likely to develop early in life. First, ultraviolet-mediated vision enhances the foraging performance in young of various fish species (yellow perch, Loew *et al.* 1993; rainbow trout and pumpkinseed, Browman *et al.* 1994). Second, the process of exogenous feeding in

salmonids can start before full absorption of the yolk sac (Thomas and Shelton, 1968; Hurley and Brannon, 1969). Hence, if the time of appearance of accessory corner cones is developmentally linked to the initiation of exogenous feeding, it may occur very soon after hatching.

The goals of this study were twofold: (1) to document the growth of all retinal layers and cone types found during early ontogeny of sockeye salmon, and (2) to measure the spectral and polarized light sensitivities of the animal prior to and after smoltification. In addition to these physiological measurements, the theoretical visual acuity of the animal was calculated as an indicator of spatial resolution and foraging capabilities.

The sockeye salmon was chosen as a study subject because of its complex life history which involves several years of residence in a nursery lake as a juvenile. This habitat is shared by rainbow trout (*Oncorhynchus mykiss*), a species that possesses a full square mosaic arrangement with accessory corner cones and ultraviolet vision at the parr stage (pre-smolt, Beaudet *et al.* 1993; see van der Meer, 1992, for possible cone configurations in fish retinas). In contrast to the rainbow trout, which remains in fresh water and undergoes a transformation somewhat similar to smoltification, the sockeye salmon smolts completely before reaching the ocean, where it resides for 1–4 years before migrating back to the natal river to spawn and die (Groot and Margolis, 1991). Since ultraviolet-mediated vision may be involved in foraging and/or orientation during migration of young salmon (Hawryshyn *et al.* 1989; Parkyn and Hawryshyn, 1993; Novales Flamarique and Hawryshyn, 1993), sockeye salmon provides an appropriate model for studying retinal development and visual sensitivities in this behavioural and ecological context.

Table 1. *Mean body dimensions of study animals*

Stage	Eye dimensions (<±0.04 mm) Long axis	Eye dimensions (<±0.04 mm) Short axis	Total body length (<±3.5 mm)	Yolk sac dimensions (<±0.85 mm) Long axis	Yolk sac dimensions (<±0.85 mm) Short axis
Embryo	1.35	1.27			
Hatch	1.37	1.48	20.15	9.06	3.65
W1	1.39	1.55	20.7	8.75	3.42
W2	1.40	1.58	21.55	8.41	3.3
W3	1.68	1.75	24.21	8.02	3.25
W4	1.75	1.85	25.1	7.93	2.82
W5	1.76	1.92	27.3	7.8	2.61
W6	1.78	2.02	27.8	7.64	2.49
W7	1.82	2.18	30.35	6.4	2.32
W8	2.01	2.19	31.2		
W10	2.07	2.33	35.6		
Parr	2.31	2.45	55.3 (3.1)		
Smolt M11	3.61	3.72	118 (12)		

Standard deviation extremes for each column are given in parentheses. The average length of parr and smolts is also specified (standard deviations are given in parentheses). The average mass of parr was 4.2±0.3 g; the average mass of smolts was 11.2±0.8 g. The eye and yolk sac dimensions correspond to the long and short axis of both structures.

W1–W10 refer to weeks 1–10 after hatching, M11 is the eleventh month after hatching; N=3.

Materials and methods

Sockeye salmon (*Oncorhynchus nerka*) were obtained at different developmental stages from Rosewall Creek hatchery (Vancouver Island, British Columbia, Canada) (Table 1). All the fish were the progeny of the same parents that had been caught in Pinkut Creek spawning channel (Babine Lake, British Columbia, Canada); eggs were fertilized at the hatchery. Embryos were raised in the dark until hatching; all post-hatching development occurred under a 12 h:12 h L:D cycle (see Fig. 3 for the spectral composition of the lamp). Fish were kept in a circular tank with flowing water at 9 °C and fed a daily diet of BioDiet Grower pellets (Bio-Products Inc., Warrenton, Oregon, USA).

Histological preparations

Seven fish from each developmental stage (except for the embryo, parr and smolt stages, Table 1) were anaesthesized by brief immersion in a 0.1 g l^{-1} solution of tricaine methanesulphonate (MS-222). They were then decapitated and the heads immersed in primary fixative (2.5 % glutaraldehyde, 1 % paraformaldehyde in 0.06 mol l^{-1} phosphate buffer, pH 7.2 at 4 °C, Ali and Anctil, 1976) for light and transmission electron microscopy. Six eggs, the yolks of which were perforated to enable rapid penetration of the fixative, were also fixed. Eyes from specimens at the parr and smolt stages were fixed following electrophysiological recordings.

Fixed retinas from six specimens at each stage were removed from the eyes while the remaining eye was treated in its entirety. The tissue was then post-fixed with osmium tetroxide, dehydrated through an ethanol series and embedded in Epon media (Ali and Anctil, 1976). Three of the retinas at each stage were sectioned radially (along the long axis of the photoreceptors) while the remaining three retinas were cut tangentially (across the width of the photoreceptors). Tissue shrinkage was estimated at 15 % by measuring differences in retinal size prior to fixation and after embedding. However, no corrections were made for shrinkage in the data presented except in the visual acuity calculations.

Histological measurements

The retina of the sockeye salmon can be divided into eight layers from the sclera to the vitreous humour (Figs 1A,B, 2): retinal pigment epithelium (RPE), visual cell layer (VCL), outer nuclear layer (ONL), outer plexiform layer (OPL), inner nuclear layer (INL), inner plexiform layer (IPL), ganglion cell layer (GCL) and nerve fibre layer (NFL). A photoreceptor square mosaic can be observed from tangential sections cut across or near the ellipsoids of the cones (Fig. 2B,C). More vitreally, the INL is made up of at least four types of cells and

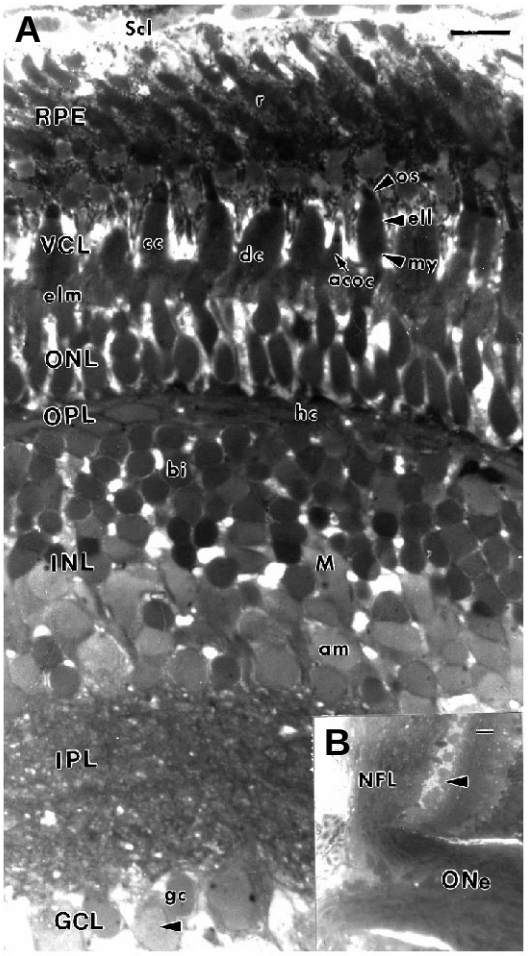

Fig. 1. (A) Radial section from a 5-week-old sockeye salmon retina (alevin stage). (B) Radial section of the optic nerve head showing the nerve fibre layer (NFL). Arrowhead points to ganglion cell layer (GCL) cell bodies, also shown in A. The NFL is thickest where axons accumulate near the optic nerve head. Scale bar, 10 μm. acoc, accessory corner cone; am, amacrine cell; bi, bipolar cell; cc, central cone; dc, double cone; ell, ellipsoid (of inner segment); gc, ganglion cell; hc, horizontal cell; M, Mueller cell; my, myoid (of inner segment); ONe, optic nerve; os, outer segment; r, rod; Scl, Sclera. Retinal layers: RPE, retinal pigment epithelium; VCL, visual cell layer; elm, external limiting membrane; ONL, outer nuclear layer; OPL, outer plexiform layer; INL, inner nuclear layer; IPL, inner plexiform layer; GCL, ganglion cell layer, NFL, nerve fibre layer.

their connections. Oriented parallel to the retinal surface are the horizontal cells (Fig. 2E); these are followed by bipolar cells (Fig. 2F) and, at the inner border of the INL, by amacrine cells (Fig. 2G). Mueller cells extend the entire length of the retina. The GCL exhibits large pale-staining ganglion cell bodies (Fig. 2H); neural dendrites and axons exiting the GCL form the NFL (Fig. 1B).

Tangential sections at the ellipsoid level of photoreceptors enabled the density of each type of cone (accessory corner cone, central cone and double cone) and the diameter of each individual type of cone to be measured. This was done by counting, for each retina, the numbers of each cone type in a 0.01 mm^2 piece of central retina adjacent to the optic nerve head (except for the smolt retina where dorsal, nasal and temporal regions were also examined). Similarly, the diameter of 10 cones of each type was measured for each retina. Averages from the three sets of values were pooled and mean densities and diameters for each type of cone computed for each developmental stage. The counts and measurements were made from semi-thin sections using a Zeiss microscope (model Universal R, 100× overall magnification) and a calibrated ocular micrometer. A cone was counted if at least half of its ellipsoid was within the perimeter of the 0.01 mm^2 area. Only the long axis of the cross section of double cones was measured.

The thickness of the retinal layers was measured from radial cross sections. The width of the RPE was measured from the outermost part of the RPE layer to the average tips of the pigment projections (see Ali, 1963). The VCL covered the distance from the external limiting membrane (elm, Fig. 1) to the tips of the double cone outer segments. The limits for the other measurements follow from the previous description of each layer and Fig. 1. Averages from sections of three retinas were calculated for each developmental stage.

Optical measurements of the sockeye eye

In addition to the specimens used for histology, three other fish were used to measure body length and the dimensions of the eye and the lens at each developmental stage (Table 1). For all specimens, except the parr and the smolts, the lens was measured with a calibrated ocular micrometer, while the other measurements were made using a Vernier caliper. From these measurements and corresponding cone density measurements, the minimum angle for stimulation of two non-neighbouring cones (α) was estimated from the formula in Tamura and Wisby (1963):

$$\sin\alpha = (1/f)\{[0.1 \times (1 + S) \times 2]/(n)^{1/2}\}, \qquad (1)$$

where f (the focal length in mm) was approximated from Matthiessen's ratio (f=2.55r, r being the radius of the lens), S is the degree of shrinkage, and n is the density of cones (in total) per 0.01 mm^2 area (Blaxter and Pattie Jones, 1967). The minimum separable angle gives an indication (given a good-quality lens, Sivak, 1990) of the visual acuity of the animal. This is an important variable as it is closely associated with the development of the retina and the brain (Rahman *et al.* 1979; Jeserich and Rahman, 1979), and thus to the potential foraging performance of the animal.

Electrophysiological recordings

Animals and recording technique

Animals were anaesthetized by immersion in MS-222 (0.1 g l^{-1}) and paralysed by Pavulon injection (pancuronium bromide, 0.038 mg g^{-1} body mass). The fish were irrigated with MS-222 solution (0.005 %) during surgery to expose the optic tectum. A local anaesthetic (tetracaine, 0.5 %) was applied to the surgical area.

A Teflon-coated silver wire electrode was inserted rostro-

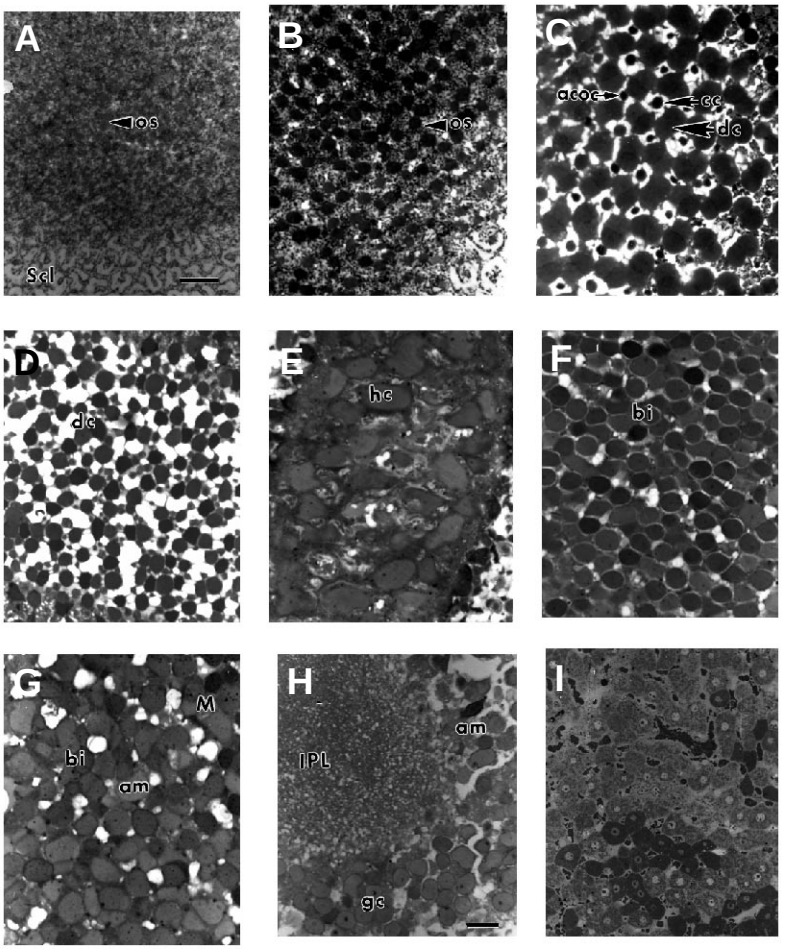

Fig. 2. Tangential sections of alevin fish retina shown in Fig. 1. (A) Scleral cells and pigment epithelium showing the first signs of (rod) outer segments. (B) Cone outer segments, a square mosaic pattern starts to appear. (C) Cone ellipsoids forming a complete square mosaic with accessory corner cones (these cones face one side of the double cone partitioning membrane). (D) Cone ellipsoids and interplexiform connections. (E) Horizontal cells. (F) Bipolar cells from the INL. (G) More vitreal part of the INL showing bipolar, Mueller and amacrine cells. (H) Mixture of IPL fibres, ganglion cells and amacrine cells. (I) Vitreal cells attached to the basal surface of the NFL. Abbreviations as in Fig. 1. Scale bar, 10 μm. Scale bar in A applies to A–G; scale bar in H applies to H and I.

ventrally through the optic tectum into the optic nerve. This electrode monitored compound action potentials from the optic nerve while a reference electrode was inserted into one of the nares of the fish and its signal subtracted from that of the recording electrode. The resulting difference signal was amplified using a Grass preamplifier (P50 series), with bandpass between 0.3 Hz and 0.1 kHz, and was displayed on an oscilloscope while simultaneously acquired by computer.

The optical system used in this study consisted of a stimulus channel (with a 300 W xenon light source, Oriel) and two background channels (using 250 W tungsten–halogen sources, EJH Spectro). The stimulus energy and spectral output were controlled by an Inconnel neutral density wedge and a monochromator. Using Corion interference filters, five types of background lighting conditions were produced so that the different cone mechanisms present in sockeye salmon could be selectively isolated and an average polarization sensitivity curve obtained (Fig. 3).

During spectral sensitivity experiments, the output from the three optical channels converged onto a diffuser placed in front of the fish's eye. This ensured an even illumination from all the channels across the entire retina. In the case of polarization sensitivity measurements, each channel had its own diffuser, and a rotatable polarizer was placed immediately following the diffuser in the stimulus channel. The channels were positioned so that the stimulus polarized light was incident on the central retina, where background radiances overlapped as much as possible. Furthermore, no light from the background channels crossed the polarizer.

Prior to testing, the fish was adapted to a particular background light for 1 h. Then 13 stimulus wavelengths ranging from 350 to 660 nm were presented to the fish in an order that precluded the adaptation of any particular cone mechanism. The stimulus duration was 750 ms. Each wavelength was presented in an increasing series of 0.2 log unit intensities. The time between stimuli in each series was 30 s. This procedure was slightly different for polarization sensitivity measurements. In this case, one wavelength was chosen for the entire experiment (λ=380 nm) and the polarizer was rotated from 0 ° to 180 ° in 30 ° increments.

Compound action potentials (CAPs) were observed at the onset and at the end of the light stimulus (ON and OFF signals, Fig. 4A). For each wavelength, the voltage amplitude of these responses was plotted against increasing radiance (Fig. 4B). A third-order polynomial function was fitted to the data points and the radiance required to elicit a 20 μV response was chosen as the threshold response. This signal level was chosen for two reasons: (1) it was very close to the absolute response threshold for all wavelengths tested (below which no response was obtained), and (2) it was in the linear part of the response curve

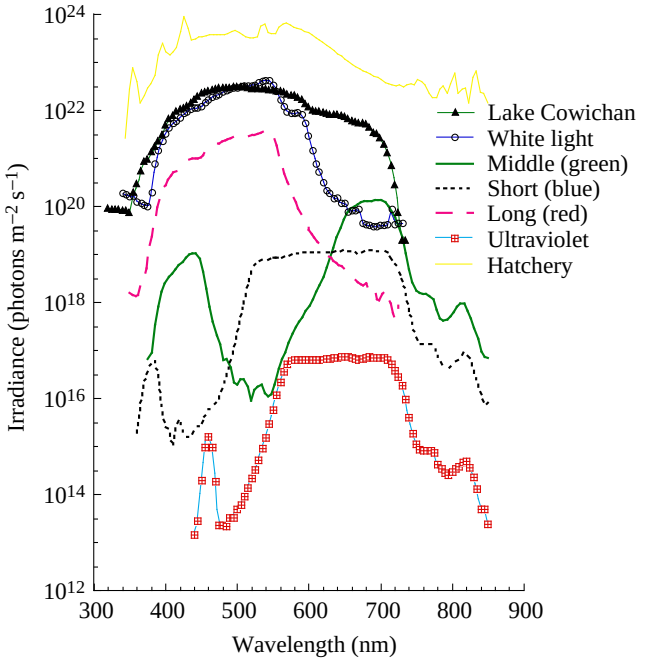

Fig. 3. Spectral characteristics of the background illuminations used to isolate the different cone mechanisms in sockeye salmon. We tried to reproduce, as white background, the downwelling spectral irradiance conditions present in Lake Cowichan at 4 m depth on 18 June 1991 at 20:42 h (Pacific Standard Time). Also shown in this figure is the spectral background during rearing conditions at the hatchery. For clarity, 1.5 log units have been added to successive graphs starting with the blue isolation condition (except for the Lake Cowichan and white light background spectra, which have the same number of log units added, i.e. 6).

(ensuring a regular and predictable response). Further details of the procedure may be obtained from Beaudet *et al.* (1993).

All animal experimentation was in accordance with guidelines set by the Canadian Council on Animal Care.

Mathematical treatment of experimental data

The Simplex curve-fitting algorithm (Caceci and Cacheris, 1984) was used to fit combinations of polynomial template curves derived by Bernard (1987; G. D. Bernard, personal communication) for vertebrate cone absorption (an eighth-order polynomial was fitted to the average rod curve). The Simplex model equation used for the cone fits was of the form (Sirovich and Abramov, 1977):

$$R = [\sum k_i A_i^p\ (\lambda)]^{1/p}, \qquad (2)$$

where R is the response curve, $A_i(\lambda)$ is the absorbance of pigment i at light of wavelength λ, and p is an exponent resulting from the mathematical requirement that the function describing the spectral sensitivity curve is differentiable at the origin (see Sirovich and Abramov, 1977). The variables k_i are differential coefficients resulting from the previous assumption. They are coupling constants that are derived from the best fit of the model to the data. The absorbance values used in the model are those of photopigments with λ_{max} at 365 nm (ultraviolet), 434 nm (short), 531 nm (middle) and 576 nm (long), as determined using microspectrophotometry (MSP) on rainbow trout cones by Hawryshyn and Hárosi (1994) (MSP data are not available for sockeye salmon). All

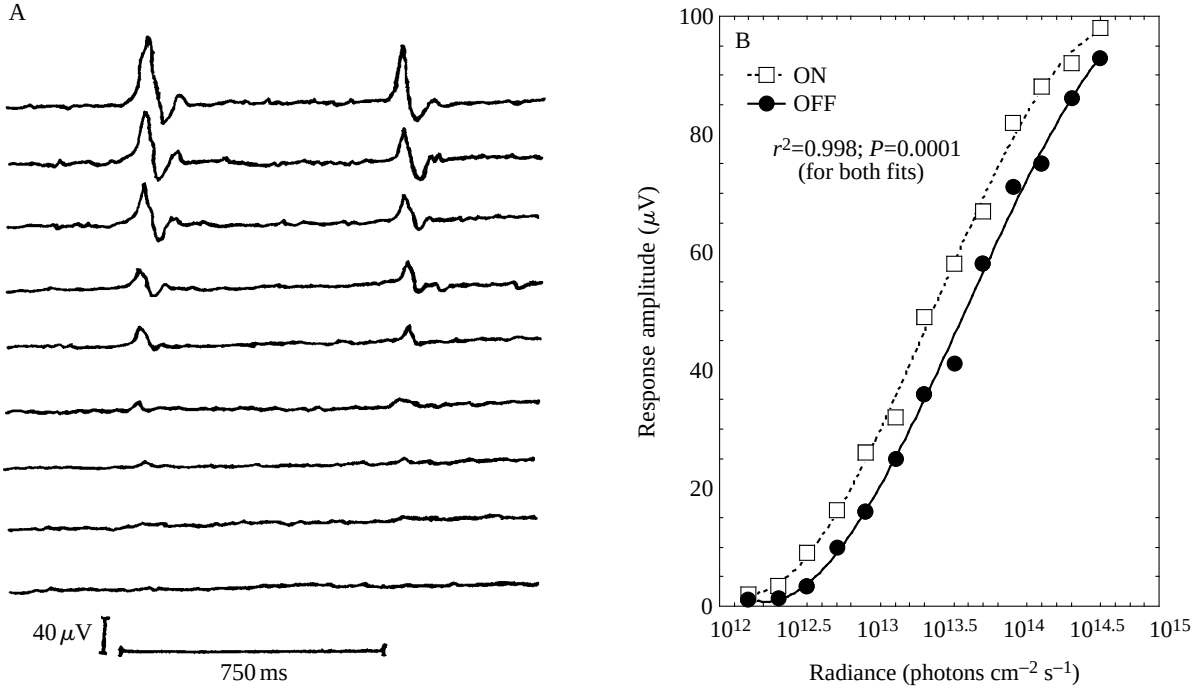

Fig. 4. (A) First nine compound action potential ON–OFF trace signals giving rise to values in B; the stimulus intensity was increased by 0.2 log units between traces. (B) Response amplitude as a function of stimulus intensity and third-order polynomial fits.

response curves that are a function of the absorbance of one or more pigments must conform to the above equation. The coupling coefficients and the exponent *p* are determined by the inputs of each photopigment to the spectral sensitivity curve and the complex interactions between photoreceptor mechanisms at various processing levels.

The procedure of fitting one best template to an isolated mechanism may give an erroneous approximation to the peak wavelength absorption of the isolated mechanism. Since isolation is never perfect, one must consider the inputs of other mechanisms that act in the spectral region examined and determine that these are significantly lower than the input of the mechanism being isolated. Thus, fitting individual polynomial templates to spectral sensitivity curves may be an oversimplification.

Results

Retinal development

Ten days prior to hatching (98 % of the fish hatched within a 2 day period 10 days after our first sampling), sockeye salmon embryos possess all five photoreceptor types present in the alevin or parr conditions (ultraviolet-, short-, middle- and long-wavelength-absorbing cones and a rod, Fig. 5A). Similarly all the retinal layers are found (Fig. 5B). Cones are arranged in a square mosaic throughout the central retina with, on average, four rods evenly dispersed around the centre cone. Photoreceptor outer segments are present in both cones and rods (Fig. 5A,C). The retina is least developed along two previously described growth zones: the embryonic fissure and near the periphery (Kunz and Callaghan, 1989).

The early growth rate of the retina is linear (Fig. 6A) and is the result of different trends followed by each retinal layer (Fig. 6B,C). The INL and GCL decrease in size during development, while the remaining layers increase in size. Cone diameters increase in size [Fig. 7A, ANOVA (model: diameter = stage conetype stage × conetype), r^2=0.997, *Pr*>*F*=0.0001, week 1 diameters are significantly different from those at hatching at α=0.05 significance level, Student–Newman–Keuls and Waller–Duncan *K*-ratio *t*-tests of means). Single cones (cc and

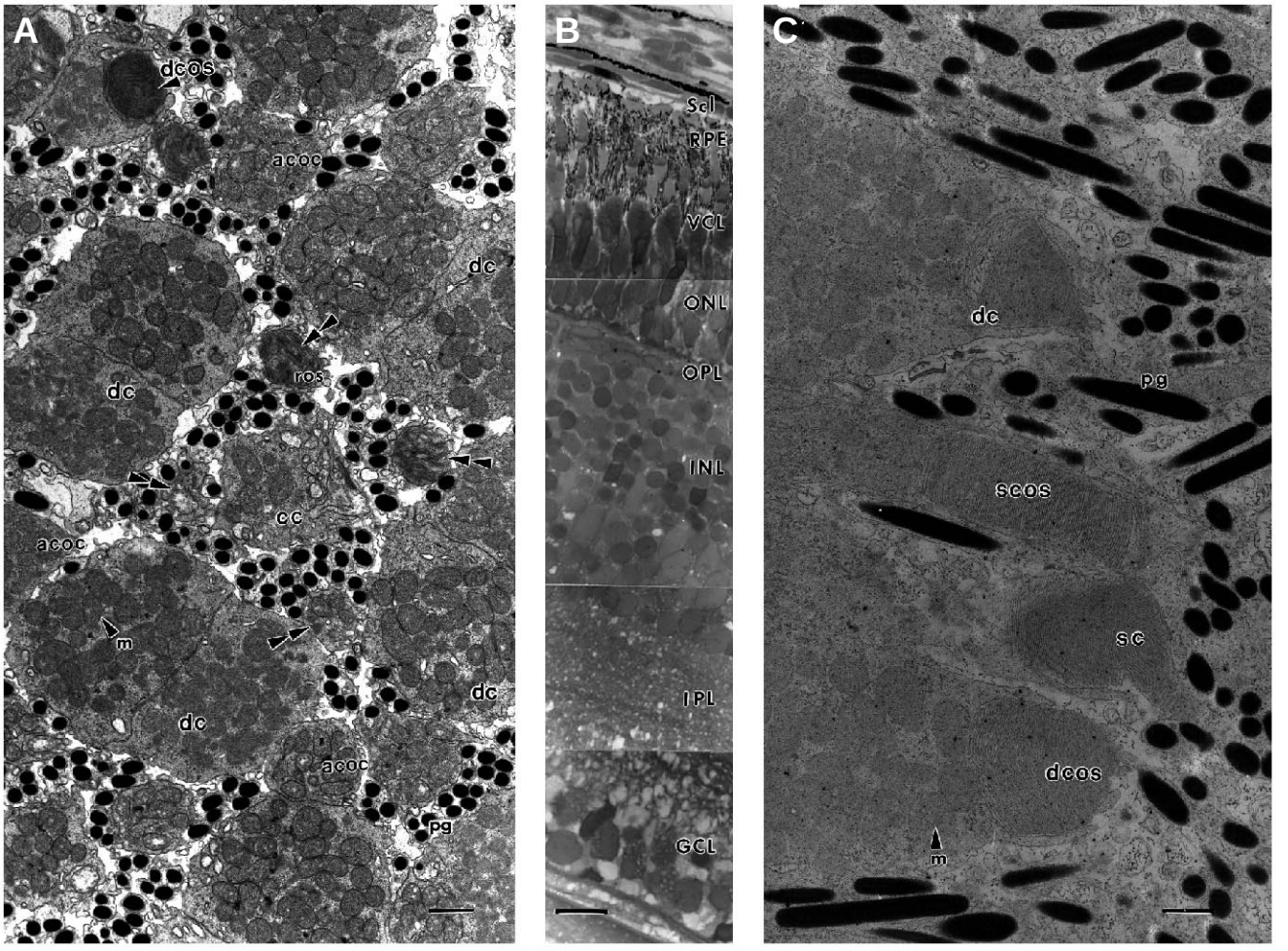

Fig. 5. (A) Tangential transmission electron micrograph section showing a complete square mosaic with four rods on average per unit mosaic (double arrowheads) in the central retina of a sockeye salmon embryo. (B) Radial section from the same fish. (C) Cone outer segments in the embryo. Abbreviations as in Figs 1 and 2; pg, pigment granule; dcos, double cone outer segment; m, mitochondria; ros, rod outer segment; sc, single cone; scos, single cone outer segment. Scale bars, A,C, 1 μm; B, 10 μm.

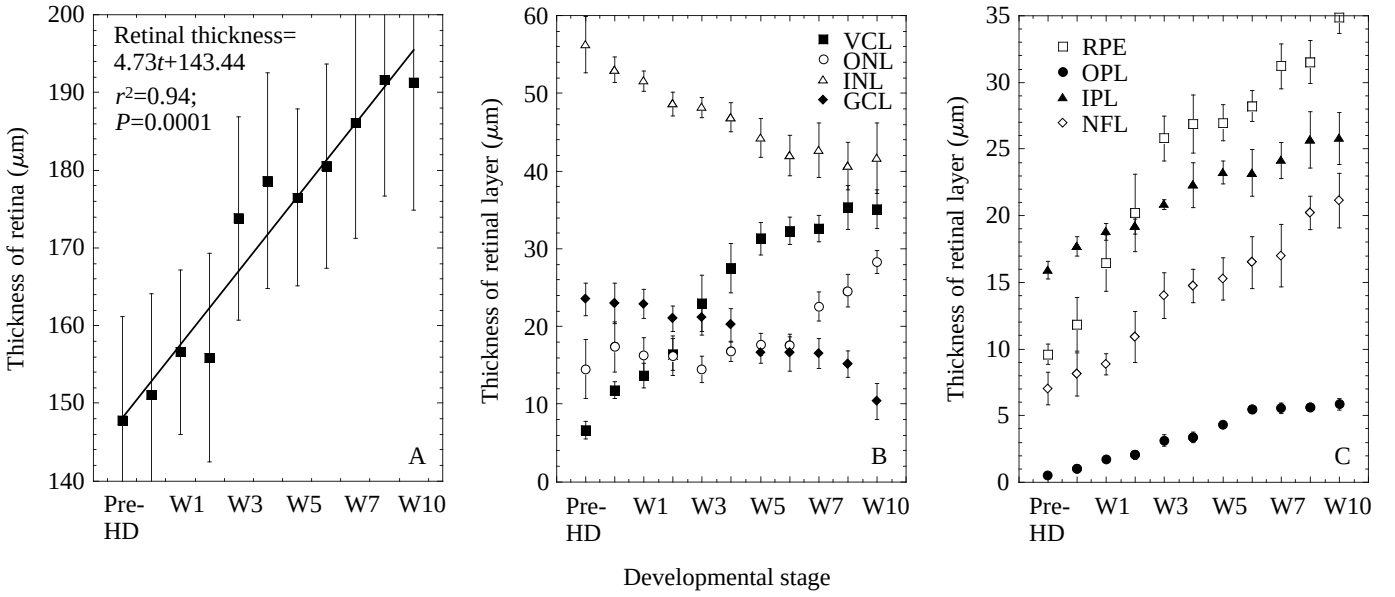

Fig. 6. (A) Growth in thickness of the entire retina during the first 10 weeks of development. (B,C) Growth of individual retinal layers (see Fig. 1 for abbreviations). Bars indicate standard errors of the means in this and all other figures (N=3 retinas per stage). Pre-HD is the pre-hatched fish (embryonic stage); W1–W10 are weeks 1–10 post-hatching.

acoc) are very similar in diameter but their tangential growth is slower than that of double cones. Cone density decreases during development [Fig. 7B, week 1 densities are significantly different from those at hatching, ANOVA (model: density = stage conetype stage × conetype), r^2=0.99, $Pr>F$=0.0001, Student–Newman–Keuls and Waller–Duncan K-ratio t-tests for means at α=0.05). This decrease is very rapid during the early stages of development but slows down from approximately week 2 post-hatching onwards. During this time, the cone pattern remains the same; however, the rod pattern is lost (see Lyall, 1957).

By the smolt stage, sockeye salmon have fewer accessory corner cones throughout most of the retina (Fig. 8, and Kunz, 1987). Areas still possessing these cones were found near the periphery and in the central retina close to the embryonic fissure. In addition to the usual cone patterns, doublet, triplet and quadruplet cone associations were found as part of incomplete square mosaics (Fig. 8A–F, see similar findings in Ahlbert, 1975). The cone mosaic, although square in most of the areas examined (especially when approaching the central retina), varied towards a row pattern in more peripheral areas and was more random immediately dorsal to

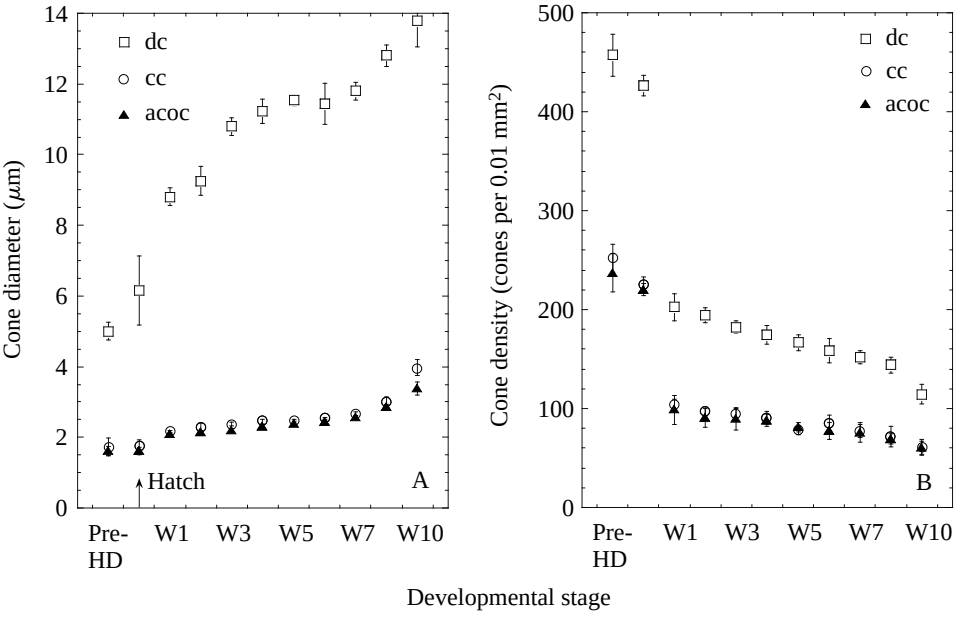

Fig. 7. (A) Tangential growth of different cone types during the first 10 weeks of development. (B) Changes in cone density for this period. Developmental stages as explained in Fig. 6. Values are means ± standard errors, N=3.

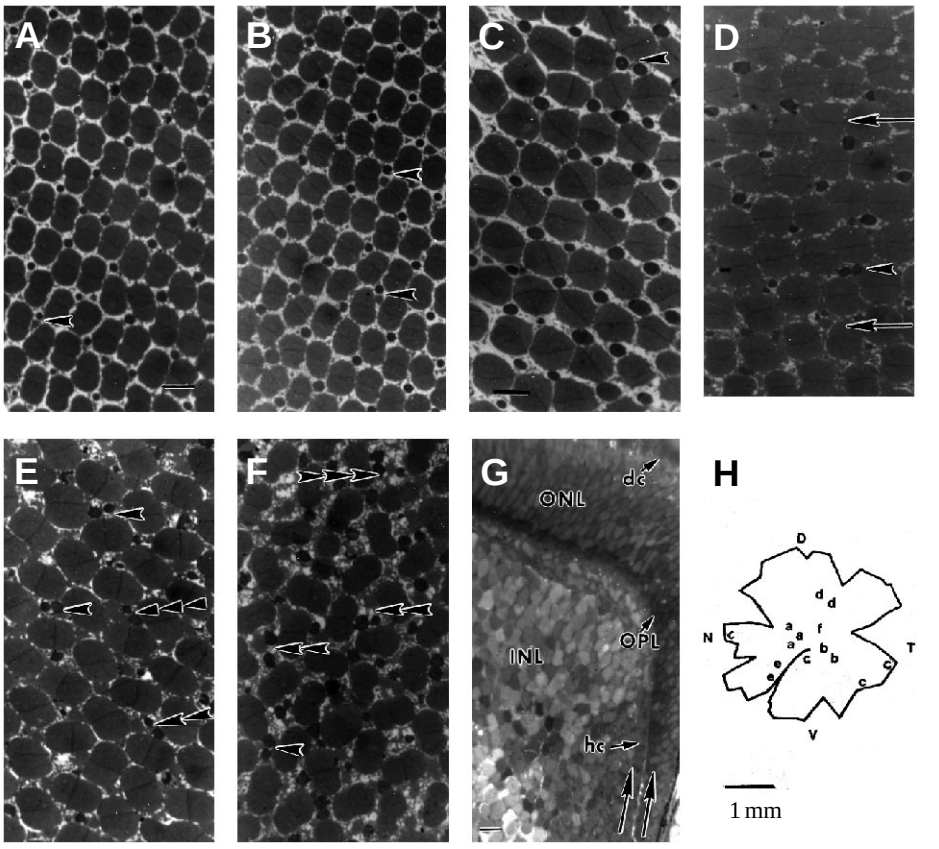

Fig. 8. Tangential sections through cone ellipsoids from different parts of the retina of smolt sockeye salmon (A–F). Single arrowheads indicate clusters of two single cones, double arrowheads indicate clusters of three single cones and triple arrowheads indicate clusters of four single cones. Arrows indicate the direction of the row pattern. (G) Radial section along the embryonic fissure showing the direction of cell proliferation (parallel arrows). From this micrograph, it can be observed that various INL-associated cells and some ONL nuclei are present early in the development of the retina. Later, horizontal cells (hc) appear, and the OPL develops thereafter. Cone nuclei are found at approximately the same developmental time as horizontal cells. These findings agree with previous observations in other fishes (Holleyfield, 1972; Nawrocki, 1985). (H) Diagram of the retina showing the position of the embryonic fissure and the locations of various mosaic types. Average double (dc) and single (sc) cone densities per 0.01 mm^2 for each location (a–f corresponding to A–F) are as follows: (A) dc, 162; sc, 86; (B) dc, 164; sc, 84; (C) dc, 118; sc, 96 (at region of central embryonic fissure); dc, 206; sc, 152 (at the dorso-temporal periphery); (D) dc, 105; sc, 64; (E) dc, 176; sc, 102; (F) dc, 108; sc, 96. Retinal thicknesses (in μm) of the different layers are as follows: RPE, 85.7; VCL, 42.6; ONL, 37.1; OPL, 5.7; INL, 40.8; IPL, 42.2; GCL, 8.4; NFL, 19.1, and total thickness is 285.7 μm. The standard errors of the mean measurements of retinal layer thickness and cone densities given above are within 16 % of the individual values. Micrographs with the same magnification are: A and B, and C–F. Scale bars in A and C, 15 μm; in H, 1 mm. N, nasal; V, ventral; D, dorsal; T, temporal.

the embryonic fissure (Fig. 8F). We know that these fish had already smolted because 30 individuals were subjected to a seawater challenge that resulted in zero mortality (see also natural smoltification ages in Groot and Margolis, 1991, p. 45).

The theoretical visual acuity of sockeye salmon improves with age [i.e. the minimum angle for stimulation of two non-neighbouring cones decreases; Fig. 9, assuming good lens quality; ANOVA (model: stage = minimum separable angle), r^2=0.938, $Pr>F$=0.0001, week 6 minimum separable angles are significantly different from those at hatching, Student–Newman–Keuls and Duncan's multiple-range tests at α=0.05]. This result parallels a decrease in total cone density and a simultaneous increase in lens radius (Fig. 9).

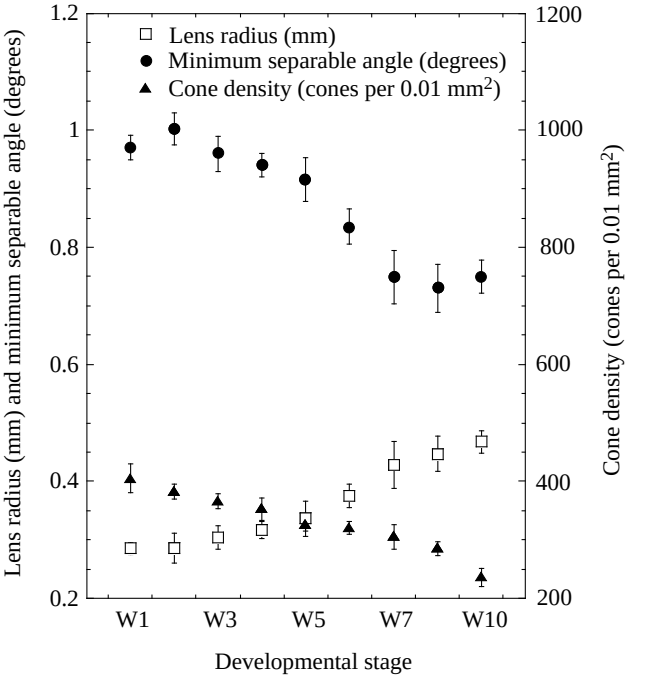

Fig. 9. The minimum separable angle for object resolution and related independent variables throughout the first 10 weeks of development. Note the decrease in minimum separable angle as the fish progressively loses its yolk sac and becomes a committed planktivore (W5–W8, see Table 1). Values are means ± standard errors of the mean (N=3).

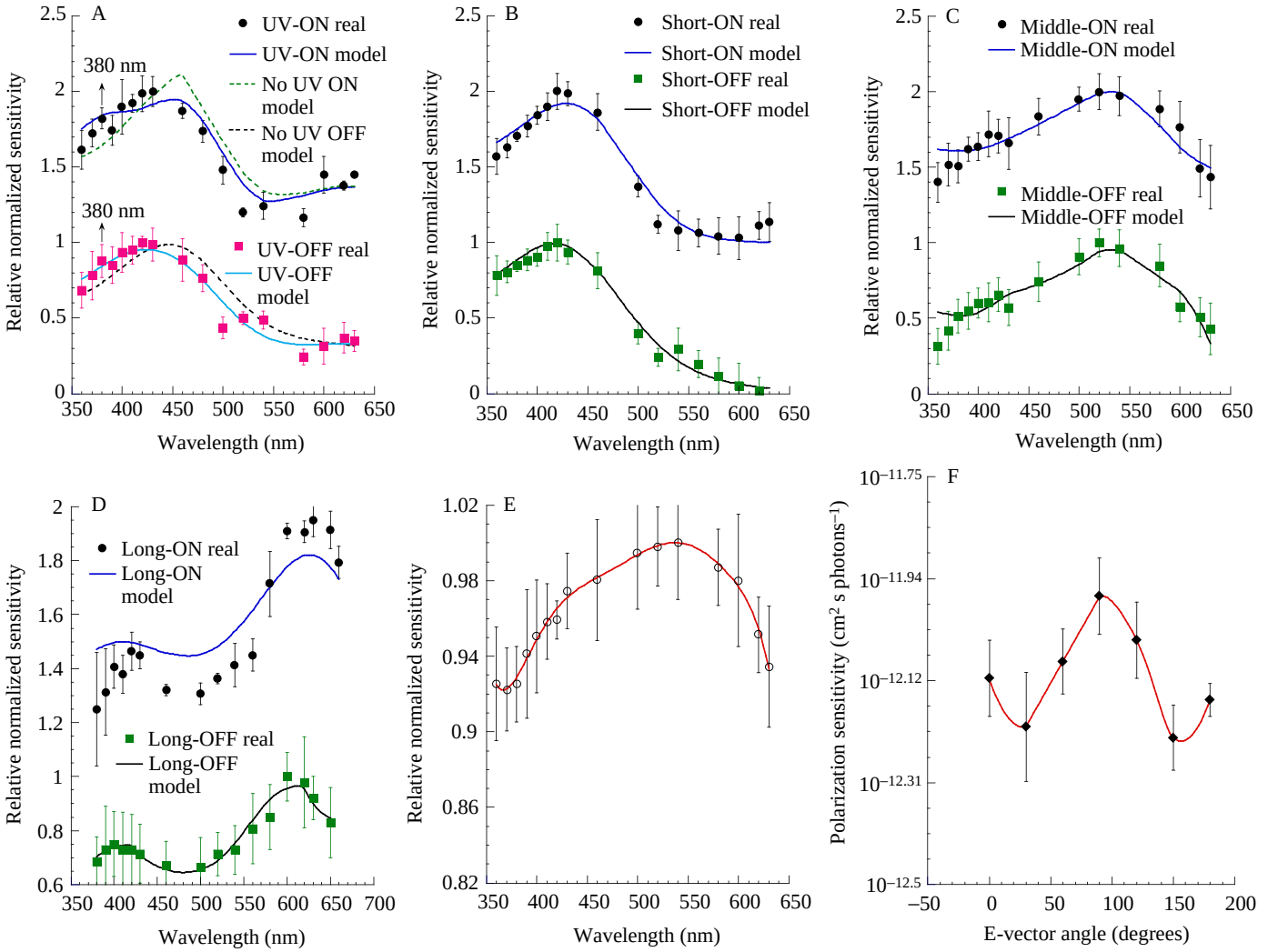

Fig. 10. (A–D) Spectral ON–OFF sensitivities of isolated cone mechanisms of sockeye salmon smolts. Vertical arrows in A indicate secondary sensitivity maxima due to an ultraviolet (UV) mechanism. Relative sensitivity values were calculated by normalizing all sensitivity values with respect to the smallest value for each of the ON and OFF responses independently and inverting the result (Bernard, 1987; G. D. Bernard, personal communication). For purposes of clarity, a value of 1 unit was added to the real and model values of ON relative sensitivity to separate them from the OFF values (real values refer to the electrophysiological data; model values for cone mechanisms were generated by the Simplex algorithm as best approximations to the real data). The bars on the curves represent the raw standard errors of the sensitivity averages (N=4 fish per mechanism). For purposes of computing the original sensitivities, we give the smallest sensitivity values (and the wavelength in nm at which they appear between parentheses) for the various mechanisms: UV-ON (430), −14.05; UV-OFF (420), −13.73; Short-ON (420), −13.35; Short-OFF (420), −13.17; Middle-ON (520), −13.32; Middle-OFF (520), −13.31; Long-ON (620), −13.75; Long-OFF (600), −14.33; Rod-ON (540), −11.54. All these values are in log(cm^2 s photons^{-1}). (E) Rod-ON spectral sensitivity under dark adaptation. (F) Sensitivity of sockeye salmon smolts (N=4) to the E-vector of polarized light under a white crepuscular background. 0 ° and 180 ° represent polarized light perpendicular to the long axis of the fish, while 90 ° is polarized light parallel to the long axis of the fish (λ=380 nm). Values are means ± standard errors of the means.

Spectral sensitivity

Under the spectral isolating backgrounds described previously, sockeye smolt ON responses revealed four types of cone mechanisms with peaks of sensitivity to ultraviolet light (λ_{max}=380 nm), blue or short-wavelength light (λ_{max}=425 nm), green or middle-wavelength light (λ_{max}=520 nm) and red or long-wavelength light (λ_{max}=635 nm) (Fig. 10). Parr exhibited similar sensitivities except for the dominance of the ultraviolet cone mechanism under ultraviolet isolation conditions (Fig. 11). When ultraviolet light was added to the ultraviolet isolation background (Fig. 10A), the peak in ultraviolet sensitivity diminished (Fig. 10B) leaving mainly a short-wavelength mechanism input (Table 2). The OFF responses follow the general shapes of the ON responses, although their spectral maxima are slightly shifted (Figs 10, 11). The OFF responses under ultraviolet isolation are driven primarily by a short-wavelength mechanism input (Figs 10A, 11; Table 2). Under scotopic conditions, the rod-driven curve showed a

Table 2. *Best-fitting Simplex-derived coefficients and least sum of squares analysis for the ON and OFF responses of the four cone mechanisms found in sockeye salmon smolts*

Neuronal mechanism response	k_1, ultraviolet	k_2, short-wavelength	k_3, middle-wavelength	k_4, long-wavelength	P	SS
UV-ON	0.406	0.856	0.002	0.082	2.48	0.15
UV-OFF	0.201	0.580	0.0002	0.443	0.70	0.06
No UV-ON	0	0.978	0.012	0.206	1.60	0.28
No UV-OFF	0	0.612	0.0003	0.527	0.49	0.19
Short-ON	0.234	0.806	0.007	0.002	0.39	0.08
Short-OFF	0.218	0.538	0.003	0.305	0.19	0.03
Middle-ON	0	0.19	0.922	0.193	2.04	0.12
Middle-OFF	0	0.106	0.771	0.001	5.82	0.12
Long-ON	0.001	0.034	0.018	0.788	1.18	0.28
Long-OFF	0.001	0.184	0.024	0.956	0.75	0.01
UV-ON (parr)	0.676	0.251	0.161	0.435	1.12	0.01
UV-OFF (parr)	0.484	0.504	0.260	0.254	1.33	0.04

Sensitivity of parr under the ultraviolet isolating background is also included.

The No UV-ON, No UV-OFF parameters correspond to best fits to the spectral sensitivity curves under ultraviolet isolation when the model is forced to discard any ultraviolet input.

SS refers to the sum of squares residual derived from the sum of the differences between mean spectral sensitivity points and those predicted by the Simplex model.

Other symbols are explained in the text.

maximum at 540 nm (Fig. 10E); however, the maximum absorbance for the mechanism is probably lower (around 525–530 nm) given the symmetry of photopigment α absorption bands. Under a white background mimicking dusk conditions in a mesotrophic lake (Novales Flamarique *et al.* 1992), sockeye salmon smolts exhibited polarization sensitivity for the ON response with maximum at a 90° E-vector angle using a 380 nm stimulus (Fig. 10F).

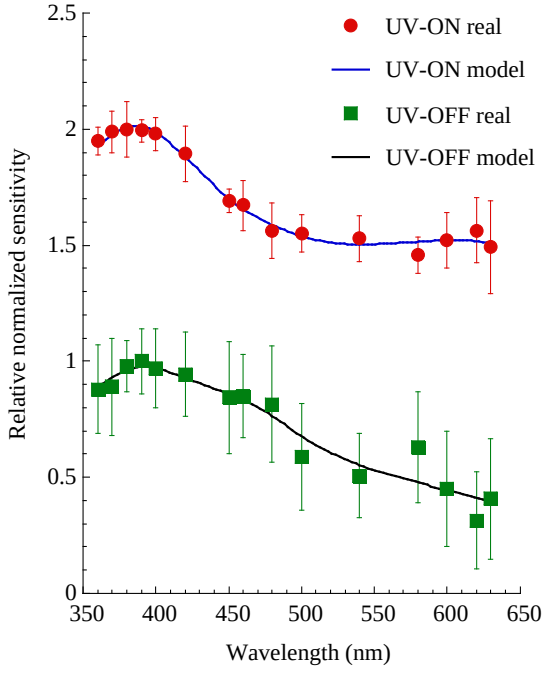

Fig. 11. Spectral ON–OFF sensitivities of parr salmon under ultraviolet (UV) isolation conditions. Treatment of data is the same as in Fig. 10. Log sensitivity maxima and associated wavelengths are: UV-ON (380), −12.51; UV-OFF (390), −12.47, where sensitivity is measured in $cm^2\,s\,photons^{-1}$. Values are means ± standard errors of the means (N=3).

Discussion

Retinal development

The presence and size of the various photoreceptor types reported in this study for pre-hatched sockeye salmon markedly differ from past findings using this and other salmonid species. Previous investigations of sockeye salmon retinal development at the light microscope level reported the absence of rods at hatching (Ali, 1959). Similar results were obtained with other species of salmon and trout (Ali, 1959, 1963; Lyall, 1957). More recently, using transmission electron microscopy, Schmitt and Kunz (1989) showed that both developing cones and rods were present in rainbow trout at hatching. These authors also reported the appearance of a cone square mosaic within the first 2 weeks after hatching (stage 3, Balon, 1975), after the cones had differentiated completely. Our results, however, show developing cones and rods arranged in a square mosaic in the central retina of the embryo (Fig. 5A,C). In addition, the photoreceptor outer segments observed at this stage are much more developed than previous ones reported for very early post-hatching stages in this and other *Oncorhynchus* species (Ali, 1959, 1963; Schmitt and Kunz, 1989). These differences in maturation rates may be population-specific as other environmental parameters in our study are similar to those reported previously (Ali, 1959; Schmitt and Kunz, 1989). However, it should be noted that O_2

concentrations, which are an important variable affecting the rate of salmonid development (Groot and Margolis, 1991), were not reported in previous studies; O_2 concentrations in this study were 11.25±0.25 p.p.m.

Rod outer segments were observed at the embryonic stage (Fig. 5A), although they appeared less developed than cone outer segments (Fig. 5C for cone outer segment lengths, rod outer segment lengths not shown in radial section). Such results also differ from those reported by Schmitt and Kunz (1989) for rainbow trout, in which rod outer segments first appeared after hatching. Nonetheless, together with observations from rainbow trout (Schmitt and Kunz, 1989), our results show that the delayed post-hatching appearance of rods reported for other teleosts does not occur in salmonids [post-hatching rod appearance occurs in the herring *Clupea harengus pallasi* (Blaxter and Pattie Jones, 1967), the zebrafish *Brachydanio rerio* (Branchek and Bremiller, 1984), the goldfish *Carassius auratus* (Raymond, 1985), the cichlid *Haplochromis burtoni* (Hagedorn and Fernald, 1992) and the walleye *Stizostedion vitreum* (Wahl, 1994)]. Pre-hatching appearance of rods has also been reported in the yellow perch (Ahlbert, 1973), as well as in some amphibians (Grant *et al.* 1980). In the European eel *Anguilla anguilla*, rods are present before cones (Pankhurst, 1984).

The growth rate of the sockeye salmon retina is linear during the early development of the animal (Fig. 6A; see also Ali, 1963, for this developmental period). The growth trend slows thereafter (Fig. 8 legend) and possibly reaches a plateau in the adult condition (Ali, 1963). The variations in thickness reported for some of the retinal layers agree with previous results for other salmonids (Lyall, 1957; Ali, 1959, 1963), other teleosts (e.g. Branchek and Bremiller, 1984; Raymond, 1985) and small mammals (Reichenbach *et al.* 1991). While the various plexiform and fibre layers thicken because of the increasing complexity of neural connections being formed, the INL decreases in thickness as the ONL and VCL grow. It is thought that 'rod-precursor' cells located in the INL migrate to the ONL, perhaps guided by Mueller cells (Raymond and Rivlin, 1987; Hagedorn and Fernald, 1992), where they give rise to rods (Raymond, 1985; Raymond and Rivlin, 1987). This mechanism would explain the inverse relationship between the thickness of the ONL and the INL during early growth (Fig. 6B). Fast incorporation of rods into the VCL and stretching of the retina during the first week post-hatching would also agree well with the precipitous drop in cone density observed during this period (Fig. 7B). However, the possibility that stretching of the retina to incorporate rods explains our results (see Hagedorn and Fernald, 1992) remains a hypothesis to be tested. This could be done by measuring the numbers of rods in square mosaics and the distances between cones in the square mosaics prior to and after rod incorporation. Nevertheless, we favour the idea of simultaneous stretching of the retina (due to eye growth) and rod incorporation in the space created.

The tight square mosaic cone arrangement present in the embryo progressively disperses as the retina grows, additional rods are added and new retina is formed along the embryonic fissure and the periphery (Fig. 8G, Kunz and Callaghan, 1989; Hagedorn and Fernald, 1992). Mean cone diameters increase during development but the entire retina expands at a faster rate. As a result, cone density decreases (Fig. 7B). Despite this, the theoretical visual acuity increases as a result of eye and lens growth which overcompensates for the decrease in cone density (Fig. 9, Blaxter and Pattie Jones, 1967; Neave, 1984; Fernald, 1991). The minimum angles of separation derived for sockeye salmon permit us to calculate the maximum distance at which a young fry (after absorption of its yolk sac, when it is approximately 3 cm in length) would locate a prey item. Considering the average prey item to be 1.20 mm in length (see Browman *et al.* 1994), the maximum distance at which it would be detected can be calculated to be 78 mm. In accordance with this prediction, maximum prey move distances for rainbow trout of this size feeding on 1.20 mm *Daphnia pulex* oscillate around 75 mm (Browman *et al.* 1994). Prey move distances refer to the average distances covered by the fish, between pauses, when it scans the surroundings looking for prey. These distances are strongly correlated with the distances at which prey are located (Bell, 1990).

The differences in tangential growth rates of the various cone types can be related to the visual ecology of sockeye salmon. Using geometrical methods, van der Meer (1992) has shown that square mosaic patterns with central elements, and with or without single 'accessory' elements (cone configurations $PAT6^{C}$ and $PAT6^{CA}$ in Fig. 4 of van der Meer, 1992), are well adapted for vision in bright and dim light. These conclusions are based on the larger area that the double cones occupy in the square mosaic (supposedly driving the luminosity system), the better cone packing that could be achieved with single and double cones as opposed to that with single cones alone, and the advantages for maximum photon catch in bright environments. In dim environments, maximization of the photon-catching abilities of double cones would lead to rearrangement of the area occupied by these at the expense of single cones, resulting in row mosaics (van der Meer, 1992). All these arguments support the contention that sockeye salmon, a fish experiencing many different light environments throughout its lifetime, should have a double cone mosaic arrangement. In the case of Babine lake salmon, limnological data suggest that these fish live in waters that can be classified as oligotrophic or mesotrophic (Narver, 1967; Hartman and Burgner, 1972). Thus, the light field to great depths should expand the full spectrum from ultraviolet to long wavelengths and be relatively bright (spectral irradiance $>10^{15}$ photons $m^{-2}\,s^{-1}$, Smith *et al.* 1973), while the lower photic zone should probably peak in the short to middle wavelengths (Novales Flamarique *et al.* 1992). Young salmon in this lake system exhibit a diel vertical migration: the fish stay at depths between 24 and 40 m during the day and within 3–5 m of the surface during crepuscular periods (Narver, 1967). Thus, the fish inhabit a variety of photic habitats where a square mosaic with predominant double cone surface area

would maximize photon catch and, indirectly, the chances of survival due to prey location and predator avoidance.

Our observations for the smolt retina showing various types of cone arrangements agree with Ahlbert's (1975) observations for other salmonid species. According to Ahlbert and other authors, the retinas of Atlantic salmon and trout shift from a full square mosaic retina at the parr stage to one with fewer accessory corner cones and more row patterns in the adult (Kunz and Callaghan, 1989; Beaudet *et al.* 1993). The cone densities found are also characteristic of the young smolt condition (Ali, 1963; Ahlbert, 1975), and their distribution implies a zooplanktivorous existence (highest densities in the ventro-temporal retina, Fig. 8, Ahlbert, 1969, 1975).

Visual sensitivity

The peak sensitivities of the ON responses of cone mechanisms found for sockeye smolts are different from those found for rainbow trout and goldfish using behavioural methods (trout maxima at 440, 535 and 630 nm, Douglas, 1983; goldfish maxima at 365, 440, 540 and 640 nm, Hawryshyn, 1991). Using a similar optic nerve recording technique, Beaudet *et al.* (1993) showed that parr rainbow trout possess an ultraviolet cone mechanism peaking at 390 nm. These authors further showed that the ultraviolet cone mechanism was lost after the fish 'pseudo-smolted' (see also Hawryshyn *et al.* 1989) and that this was accompanied by a loss of accessory corner cones in the central retina. Our results provide evidence of ultraviolet sensitivity in smolt sockeye salmon from the presence of a residual maximum peaking at 380 nm under ultraviolet isolating conditions (Figs 10A, 11). This peak is indeed driven by the ultraviolet mechanism since it diminishes when ultraviolet light is introduced into the background illumination (Fig. 10B; Table 2). This conclusion is also supported mathematically as the fit becomes much worse if the model does not take into consideration the input from an ultraviolet cone mechanism (Fig. 10A, see SS in Table 2). In addition, β band contributions from the middle- and long-wavelength mechanisms under ultraviolet isolating conditions are by comparison much smaller (Table 2), as would be expected since the main peaks of these two mechanisms are below the sensitivities observed in the ultraviolet range, and β bands are at least 0.5 log units below the main peaks (Fig. 10C,D; Beauchamp and Lovasik, 1973).

The difference between these results and those of Beaudet *et al.* (1993) may be due to differences in the visual systems of the species studied. However, we believe that a more likely explanation resides in the fact that a diffuser was used to obtain spectral sensitivity curves in the present study. Beaudet *et al.* (1993) were stimulating preferentially the centro-ventral retina while, with a diffuser, we were stimulating all regions of the retina. Our results, therefore, suggest that a population of ultraviolet cones remains functional in the retina (Fig. 8), which may partly explain why ultraviolet single units are found in the torus semicircularis of large juvenile rainbow trout (Coughlin and Hawryshyn, 1994).

The use of a diffuser, however, does not explain why sockeye smolts exhibit polarization sensitivity while 'pseudo-smolted' rainbow trout do not (Fig. 10F, Hawryshyn *et al.* 1990; Parkyn and Hawryshyn, 1993). The differences in this instance may be due to the larger size of the post 'pseudo-smolted' fish tested by Parkyn and Hawryshyn (1993) (50–78 g), compared with our fish (Table 1, i.e. the retina may progressively get rid of more ultraviolet cones with time after smoltification). Alternatively, as with the spectral sensitivity results, the differences may reside within the visual genetic make-up of each species.

The peak OFF responses of the middle- and long-wavelength mechanisms differ from those of goldfish (DeMarco and Powers, 1991) but resemble those of rainbow trout (Beaudet *et al.* 1993). In contrast to results found for goldfish (DeMarco and Powers, 1991), the short-wavelength mechanism input of sockeye smolts dominates the OFF response under short-wavelength and ultraviolet isolation conditions. The Simplex model nevertheless predicts a smaller input from the middle- or long-wavelength mechanisms under 'unfavourable' ultraviolet or short-wavelength isolation conditions (Table 2), which suggests that these inputs may be important components of the OFF response under natural illumination. However, it is the peak OFF response of the middle-wavelength mechanism as well as the peak rod ON response that are within the spectral maxima of wavelengths penetrating meso-eutrophic lakes (Novales Flamarique *et al.* 1992). These neuronal pathways may therefore be the major constituents of a shadow detector mechanism permitting prey detection against the downwelling light in bright and dim environments, as suggested by Beaudet *et al.* (1993).

The ecological advantages of ultraviolet vision for prey detection and orientation have been discussed in various studies (e.g. Bowmaker and Kunz, 1987; Hawryshyn *et al.* 1989; Loew and Wahl, 1991). Some of these advantages probably apply to the Babine Lake system where the majority of sockeye salmon performing the diel migration are yearlings (supposedly ultraviolet-sensitive) following copepod and *Daphnia* prey (Scarsbrook *et al.* 1978). If our results also hold for adult fish, polarized ultraviolet light may be used by the fish in the open ocean to orient towards feeding grounds or during homeward migration (Kunz and Callaghan, 1989; Hawryshyn *et al.* 1990; Novales Flamarique and Hawryshyn, 1993). Such use is probably more meaningful than outward migration from lakes, given the scarcity of environmental cues in the former environment. However, it is only in lakes that migratory observations have been extensively investigated for correlation purposes (Johnson and Groot, 1963; Groot, 1965; Dill, 1971).

We wish to thank Mr Luc Beaudet for technical help and Mr William Harrower for the sockeye specimens. We would also like to thank Dr Dave Coughlin for his version of the Simplex program. Dr Christina Wahl-Loew, Luc Beaudet and Daryl Parkyn provided valuable comments on the manuscript. This research was supported by a NSERC operating grant to C.W.H. and graduate scholarships to I.N.F.; I.N.F. was supported by a

NSERC postgraduate scholarship and by a University of Victoria President's Research Award.

References

AHLBERT, I.-B. (1969). The organization of the cone cells in the retinae of four teleosts with different feeding habits (*Perca uviatilis* L., *Lucioperca lucioperca* L., *Acerina cernua* L. and *Coregonus albula* L.). *Ark. Zool.* **22**, 445–481.

AHLBERT, I.-B. (1973). Ontogeny of double cones in the retina of perch fry (*P. fluviatilis*, Teleostei). *Acta zool. (Stockh.)* **54**, 241–254.

AHLBERT, I.-B. (1975). Organization of the cone cells in the retinae of Salmon (*Salmo salar*) and Trout (*Salmo trutta trutta*) in relation to their feeding habits. *Acta zool. (Stockh.)* **57**, 13–35.

ALI, M. A. (1959). The ocular structure, retinomotor and photobehavioural responses of juvenile Pacific salmon. *Can. J. Zool.* **37**, 965–996.

ALI, M. A. (1963). Correlation of some retinal and morphological measurements from the Atlantic salmon (*Salmo salar*). *Growth* **27**, 57–76.

ALI, M. A. AND ANCTIL, M. (1976). *The Retinas of Fishes: An Atlas*. Berlin: Springer.

ALI, M. A. AND WAGNER, H. J. (1980). Vision in charrs: a review and perspectives. In *Perspectives in Vertebrate Science*, vol. 1 (ed. E. K. Balon), pp. 391–422. The Hague, The Netherlands: Dr W. Junk bv Publishers.

BALON, E. K. (1975). Terminology of intervals in fish development. *J. Fish. Res. Bd Can.* **32**, 1663–1670.

BEAUCHAMP, R. D. AND LOVASIK, J. V. (1973). Blue mechanism response of single golfish optic fibers. *J. Neurophysiol.* **36**, 925–939.

BEAUDET, L., BROWMAN, H. I. AND HAWRYSHYN, C. W. (1993). Optic nerve response and retinal structure in rainbow trout of different sizes. *Vision Res.* **33**, 1739–1746.

BELL, W. J. (1990). *Searching Behaviour. The Behavioural Ecology of Finding Resources.* New York: Chapman & Hall. 400pp.

BERNARD, G. D. (1987). Spectral characterization of butterfly L-receptors using extended Dartnall/McNichol template functions. *J. opt. Soc. Am.* A, series 2, **4**, 123.

BLAXTER, J. H. S. (1975). The eyes of larval fish. In *Vision in Fishes* (ed. M. A. Ali), pp. 427–444. New York: Plenum Press.

BLAXTER, J. H. S. AND PATTIE JONES, M. (1967). The development of the retina and retinomotor responses in the herring. *J. mar. biol. Ass. U.K.* **47**, 677–697.

BOWMAKER, J. K. AND KUNZ, Y. W. (1987). Ultraviolet receptors, tetrachromatic colour vision and retinal mosaics in brown trout (*Salmo trutta*): Age dependent changes. *Vision Res.* **27**, 2101–2108.

BRANCHEK, T. AND BREMILLER, R. (1984). The development of photoreceptors in the zebrafish, *Brachydanio rerio*. I. Structure. *J. comp. Neurol.* **224**, 107–115.

BROWMAN, H. I., NOVALES FLAMARIQUE, I. AND HAWRYSHYN, C. W. (1994). Ultraviolet photoreception contributes to the foraging performance of two species of zooplanktivorous fishes. *J. exp. Biol.* **186**, 187–198.

CACECI, M. S. AND CACHERIS, W. P. (1984). Fitting curves to data, the Simplex algorith is the answer. *Byte* **5**, 340–360.

CARTER-DAWSON, L. D. AND LA VAIL, M. M. (1979). Rods and cones in the mouse retina. II. Autoradiographic analysis of cell generation using tritiated thymidine. *J. comp. Neurol.* **188**, 263–272.

COUGHLIN, D. J. AND HAWRYSHYN, C. W. (1994). Ultraviolet sensitivity in the torus semicircularis of rainbow trout (*Oncorhynchus mykiss*). *Vision Res.* **34**, 1407–1413.

DEMARCO, P. J. AND POWERS, M. K. (1991). Spectral sensitivity of ON and OFF responses from the optic nerve of goldfish. *Vis. Neurosci.* **6**, 207–217.

DILL, P. A. (1971). Perception of polarized light by yearling sockeye salmon (*Oncorhynchus nerka*). *J. Fish. Res. Bd Can.* **28**, 1319–1332.

DOUGLAS, R. H. (1983). Spectral sensitivity of rainbow trout (*Salmo gairdneri*). *Rev. Can. Biol. exp.* **42**, 117–122.

FERNALD, R. D. (1991). Teleost vision: seeing while growing. *J. exp. Zool.* (Suppl.) **5**, 167–180.

GRANT, P., RUBIN, E. AND CIMA, C. (1980). Ontogeny of the retina and optic nerve in *Xenopus laevis*. I. Stages in the early development of the retina. *J. comp. Physiol.* **189**, 593–613.

GROOT, C. (1965). On the orientation of sockeye salmon (*Oncorhynchus nerka*) during seaward migration out of lakes. *Behaviour* (Suppl.), **14**, 105–158.

GROOT, C. AND MARGOLIS, L. (1991). *Pacific Salmon Life Histories*, pp. 3–117. Vancouver, BC: UBC Press.

HAGEDORN, M. AND FERNALD, R. D. (1992). Retinal growth and cell addition during embryogenesis in the teleost, *Haplochromis burtoni*. *J. comp. Neurol.* **321**, 193–208.

HARTMAN, W. L. AND BURGNER, R. L. (1972). Limnology and fish ecology of sockeye salmon nursery lakes of the world. *J. Fish. Res. Bd Can.* **29**, 699–715.

HAWRYSHYN, C. W. (1991). Light-adaptation properties of the ultraviolet-sensitive cone mechanism in comparison to the other receptor mechanisms of goldfish. *Vis. Neurosci.* **6**, 293–301.

HAWRYSHYN, C. W., ARNOLD, M. G., BOWERING, E. AND COLE, R. L. (1990). Spatial orientation of rainbow trout to plane-polarized light: The ontogeny of E-vector discrimination and spectral sensitivity characteristics. *J. comp. Physiol.* A **166**, 565–574.

HAWRYSHYN, C. W., ARNOLD, M. G., CHIASSON, D. J. AND MARTIN, P. C. (1989). The ontogeny of ultraviolet photosensitivity in rainbow trout (*Salmo gairdneri*). *Vis. Neurosci.* **2**, 247–254.

HAWRYSHYN, C. W. AND HÁROSI, F. I. (1994). Spectral characteristics of visual pigments in rainbow trout (*Oncorhynchus mykiss*). *Vision Res.* **34**, 1385–1392.

HOLLEYFIELD, J. G. (1972). Histogenesis of the retina in the Killifish, *Fundulus heteroclitus*. *J. comp. Neurol.* **144**, 373–380.

HURLEY, D. A. AND BRANNON, E. L. (1969). The effect of feeding before and after yolk absorption on the growth of sockeye salmon. *Int. Pacific salmonid Fish. Commission Progress Report* **21**, 19pp.

JESERICH, G. AND RAHMAN, H. (1979). Effect of light deprivation on fine structural changes in the optic tectum of the rainbow trout (*Salmo gairdneri* Rich.) during ontogenesis. *Dev. Neurosci.* **2**, 19–24.

JOHNSON, W. E. AND GROOT, C. (1963). Observations on the migration of young sockeye salmon (*Oncorhynchus nerka*) through a large, complex lake system. *J. Fish. Res. Bd Can.* **20**, 919–934.

KUNZ, Y. W. (1987). Tracts of putative UV receptors in the retina of the two-year-old brown trout (*Salmo trutta*) and the Atlantic salmon (*Salmo salar*). *Experientia* **43**, 1202–1204.

KUNZ, Y. W. AND CALLAGHAN, E. (1989). Embryonic fissures in teleost eyes and their possible role in the detection of polarized light. *Trans. Am. Fish. Soc.* **118**, 195–202.

KUSMIC, C., BARSANTI, L., PASSARELLI, V. AND GUALTIERI, P. (1993). Photoreceptor morphology and visual pigment content in the pineal

organ and in the retina of juvenile and adult trout, *Salmo irideus*. *Micron* **24**, 279–286.

LOEW, E. R., MCFARLAND, W. N., MILLS, E. L. AND HUNTER, D. (1993). A chromatic action spectrum for planktonic predation by juvenile yellow perch, *Perca flavescens*. *Can. J. Zool.* **71**, 384–386.

LOEW, E. R. AND WAHL, C. W. (1991). A short-wavelength sensitive cone mechanism in juvenile yellow perch, *Perca flavescens*. *Vision Res.* **31**, 353–360.

LYALL, A. H. (1957). The growth of the trout retina. *Q. Jl microsc. Sci.* **98**, 101–110.

NARVER, D. W. (1967). Primary productivity in the Babine lake system, British Columbia. *J. Fish. Res. Bd Can.* **24**, 2045–2052.

NAWROCKI, L. W. (1985). Development of the neural retina in the zebrafish, *Brachydanio rerio*. PhD thesis, University of Oregon, Ann Arbor.

NEAVE, D. A. (1984). The development of visual acuity in larval plaice (*Pleuronectes platessa* L.) and turbot (*Scophthalmus maximus* L.). *J. exp. Biol. Ecol.* **78**, 167–175.

NOVALES FLAMARIQUE, I. AND HAWRYSHYN, C. W. (1993). Spectral characteristics of salmonid migratory routes from southern Vancouver Island (British Columbia). *Can. J. Fish. aquat. Sci.* **50**, 1706–1716.

NOVALES FLAMARIQUE, I., HENDRY, A. AND HAWRYSHYN, C. W. (1992). The photic environment of a salmonid nursery lake. *J. exp. Biol.* **169**, 121–141.

PANKHURST, N. W. (1984). Retinal development in larval and juvenile European eel, *Anguilla anguilla* (L.). *Can. J. Zool.* **62**, 335–343.

PARKYN, D. C. AND HAWRYSHYN, C. W. (1993). Polarized light sensitivity in rainbow trout (*Oncorhynchus mykiss*): characterization from multiunit responses in the optic nerve. *J. comp. Physiol.* A **172**, 493–500.

RAHMAN, H., JESERICH, G. AND ZEUTZIUS, I. (1979). Ontogeny of visual acuity of rainbow trout under normal conditions and light deprivation. *Behaviour* **68**, 315–322.

RAYMOND, P. A. (1985). Cytodifferentiation of photoreceptors in larval goldfish: delayed maturation of rods. *J. comp. Neurol.* **236**, 90–105.

RAYMOND, P. A. AND RIVLIN, P. K. (1987). Germinal cells in the goldfish retina that produce rod photoreceptors. *Dev. Biol.* **122**, 120–138.

REH, T. A. (1991). Determination of cell fate during retinal histogenesis: intrinsic and extrinsic mechanisms. In *Development of the Visual System, Proceedings of the Retina Research Foundation Symposia*, vol. 3 (ed. M.-K. Lam and C. J. Shatz), pp. 79–94. Cambridge, MA: The MIT Press.

REICHENBACH, A., SCHNITZER, J., FRIEDRICH, A., ZIEGERT, W., BRUCKNER, G. AND SCHOBER, W. (1991). Development of the rabbit retina. I. Size of eye and retina and postnatal cell proliferation. *Anat. Embryol.* **183**, 287–297.

SCARSBROOK, J. R., MILLER, P. L., HUME, J. M. AND MCDONALD, J. (1978). Purse seine catches of sockeye salmon (*Oncorhynchus nerka*) and other species of fish at Babine Lake, British Columbia, 1977 (data record). *Fisheries and Marine Service, Pacific Biological Station, Nanaimo, BC, Canada. Data report* **69**, 41pp.

SCHMITT, E. AND KUNZ, Y. W. (1989). Retinal morphogenesis in the rainbow trout, *Salmo gairdneri*. *Brain Behav. Evol.* **34**, 48–64.

SIROVICH, L. AND ABRAMOV, I. (1977). Photopigments and pseudopigments. *Vision Res.* **17**, 5–16.

SIVAK, J. G. (1990). Optical variability of the fish lens. In *The Visual System of Fish* (ed. R. H. Douglas and M. B. A. Djamgoz), pp. 64–80. London: Chapman & Hall.

SMITH, R. C., TYLER, J. E. AND GOLDMAN, C. R. (1973). Optical properties and color of Lake Tahoe and Crater Lake. *Limnol. Oceanogr.* **18**, 189–199.

TAMURA, T. AND WISBY, W. J. (1963). The visual sense of pelagic fishes especially the visual axis and accommodation. *Bull. mar. Sci. Gulf Caribbean* **13**, 433–438.

THOMAS, A. E. AND SHELTON, J. M. (1968). Operation of Abernathy channel for incubation of salmon eggs. *U.S. Wildlife Service, Bureau of Sport Fisheries and Wildlife, Technical Paper* **23**. 19pp.

VAN DER MEER, H. J. (1992). Constructional morphology of photoreceptor patterns in percomorph fish. *Acta biotheoretica* **40**, 51–85.

WAHL, C. M. (1994). Periodic cone cell twists in the walleye, *Stizosteidon vitreum*; a new type of retinomotor activity. *Vision Res.* **34**, 11–18.